Electronic Supplementary Material (ESI) for Dalton Transactions.
This journal is © The Royal Society of Chemistry 2014

Synthesis, Spectroscopic and Electrochemical Studies of Phosphoryl and Carbomethoxyphenyl Substituted Corroles and their Anion Detection Properties

*Pinky Yadav and Muniappan Sankar**

Department of Chemistry, Indian Institute of Technology Roorkee, Roorkee – 247667, India

Supporting information

Table of Contents (TOC)

Fig. S1 Optical absorption spectra of **3**, **3a** and **3b** in CH_2Cl_2 at room temperature

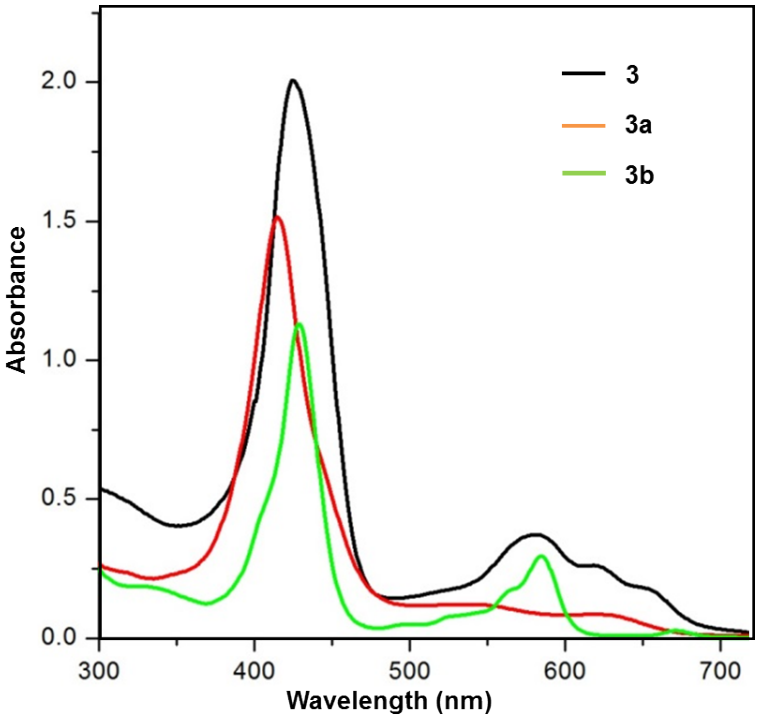

Fig. S2 ^{1}H NMR spectrum of free base 5,10,15-tris(4-diethoxyphosphorylphenyl)corrole (**2**) in $CDCl_3$

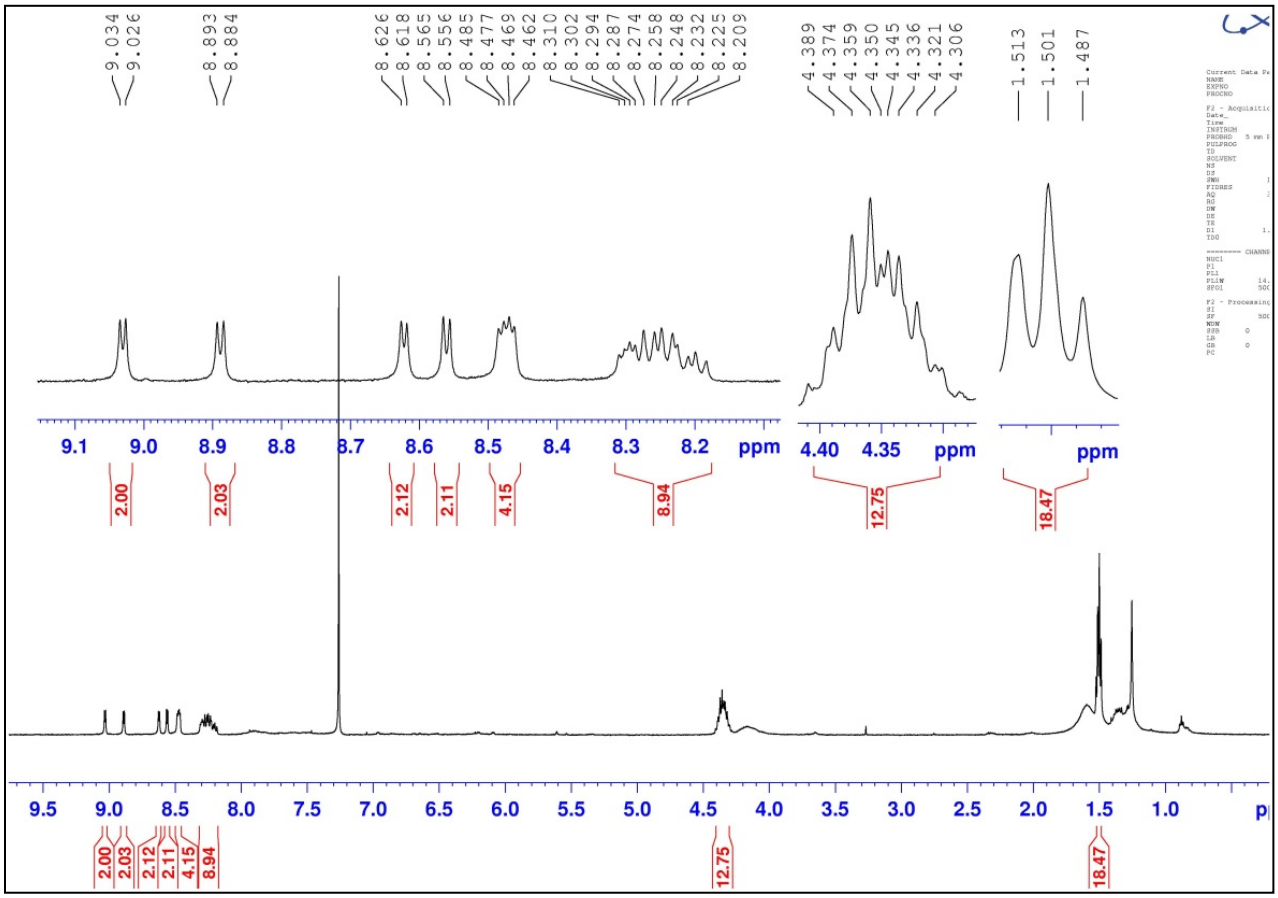

Fig. S3 ^{1}HNMR of 5,10,15-tris(4-diethoxyphosphorylphenyl)corrolato Cu(III) (**2a**) in $CDCl_3$

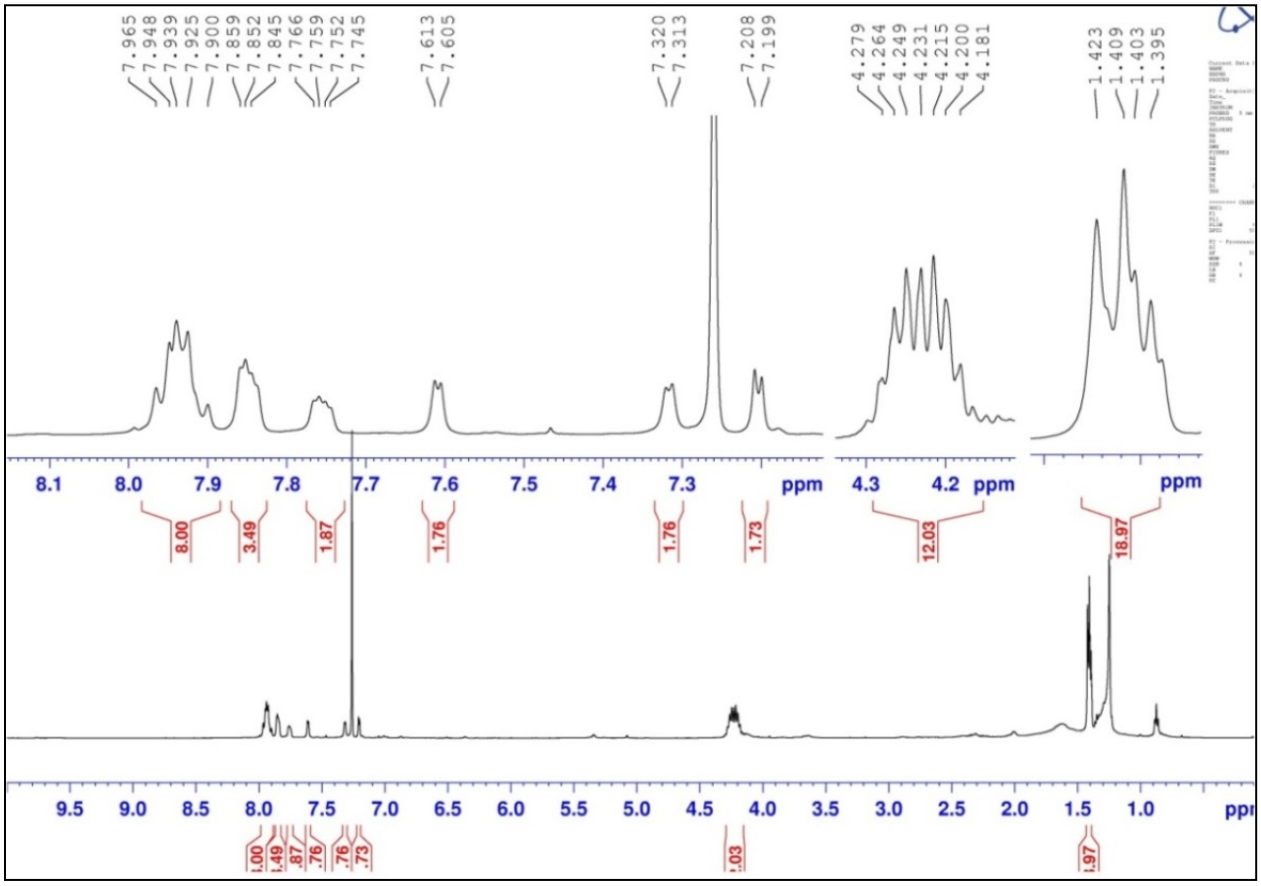

Fig. S4 ^{1}HNMR of 5,10,15-tris(4-diethoxyphosphorylphenyl)corrolato Ag(III) (**2b**) in $CDCl_3$

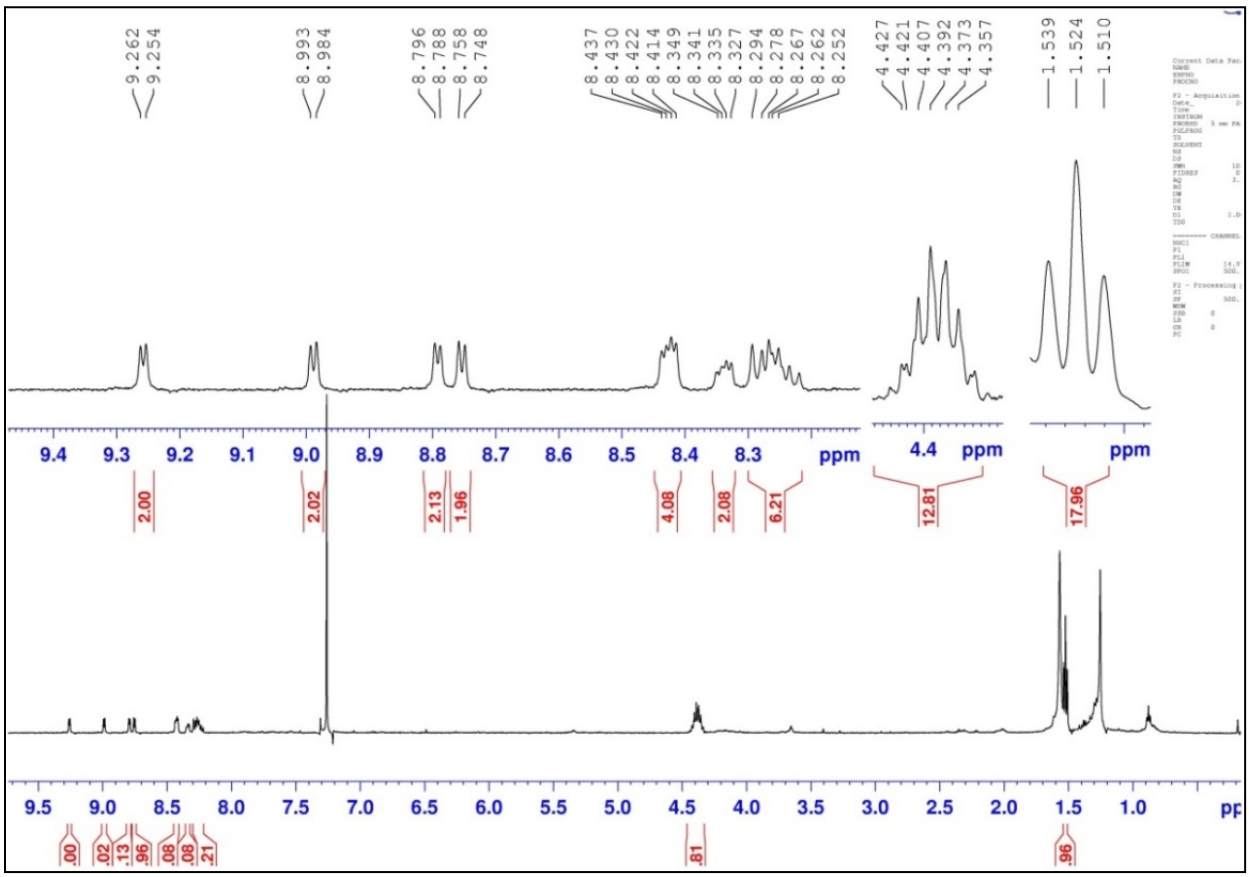

Fig. S5 ^{1}HNMR spectrum of 5,10,15-tris(4-carbomethoxyphenyl)corrolato Ag(III) (**3b**) in $CDCl_3$

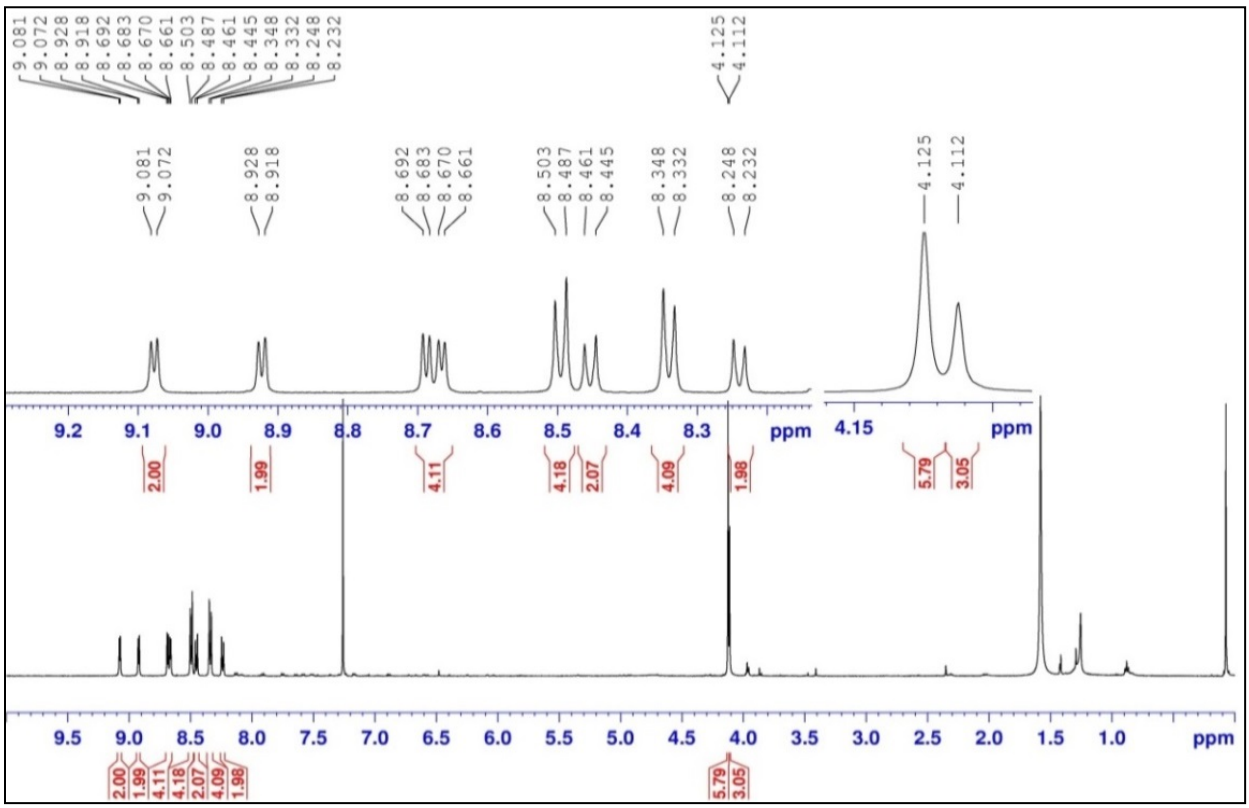

Fig. S6 MALDI-TOF Mass spectrum of **2a** (inset show the experimental and simulated isotopic pattern for $[M]^+$).

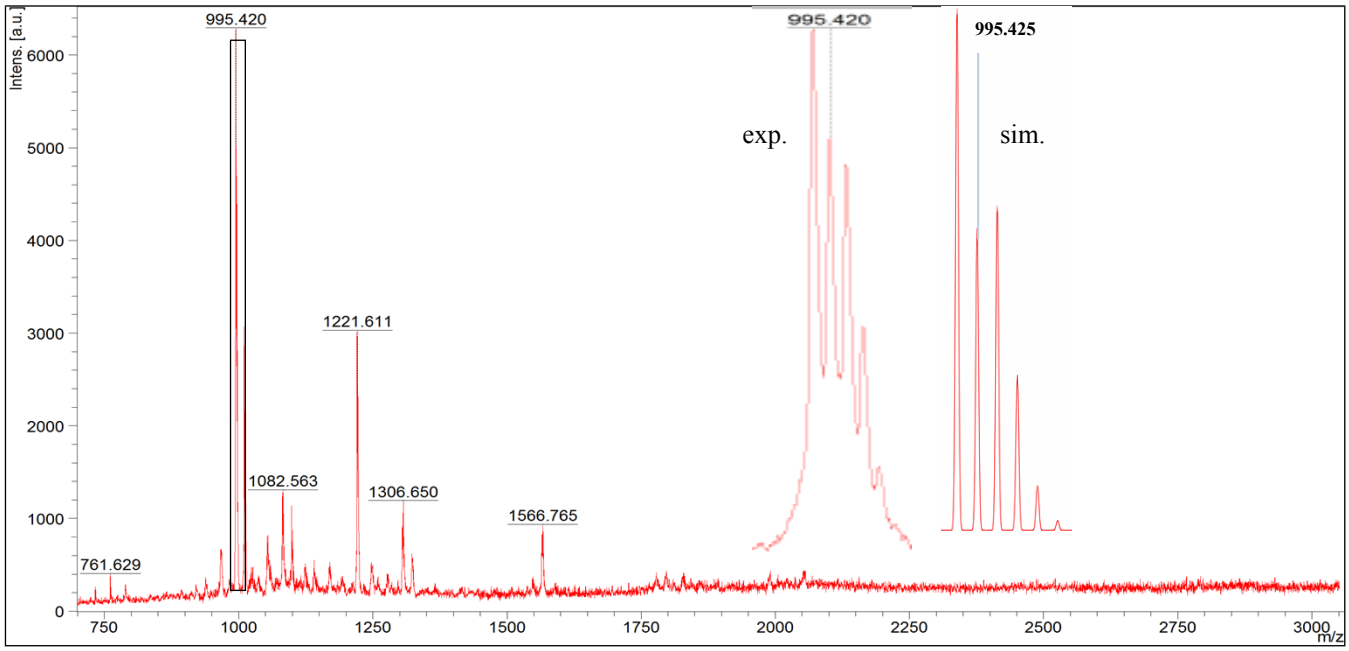

Fig. S7 MALDI-TOF Mass spectrum of **2b** (inset show the experimental and simulated isotopic pattern for $[M•H_2O]^+$).

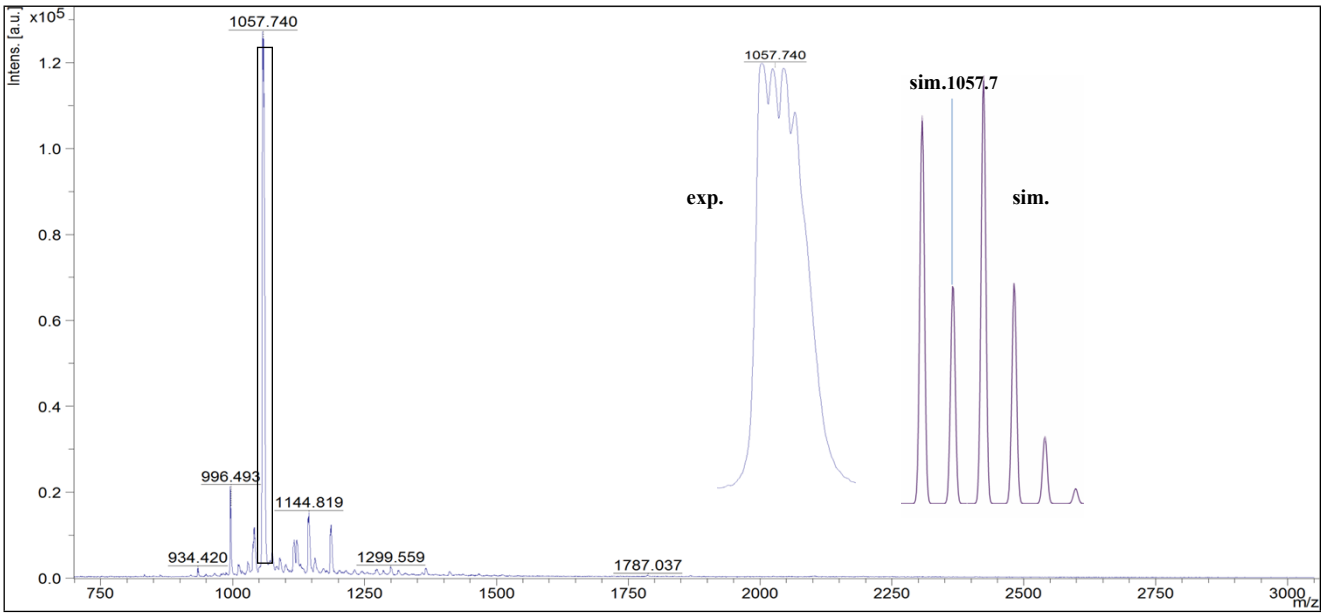

Fig. S8 MALDI-TOF Mass spectrum of **3a** (inset show the experimental and simulated isotopic pattern for $[M]^+$).

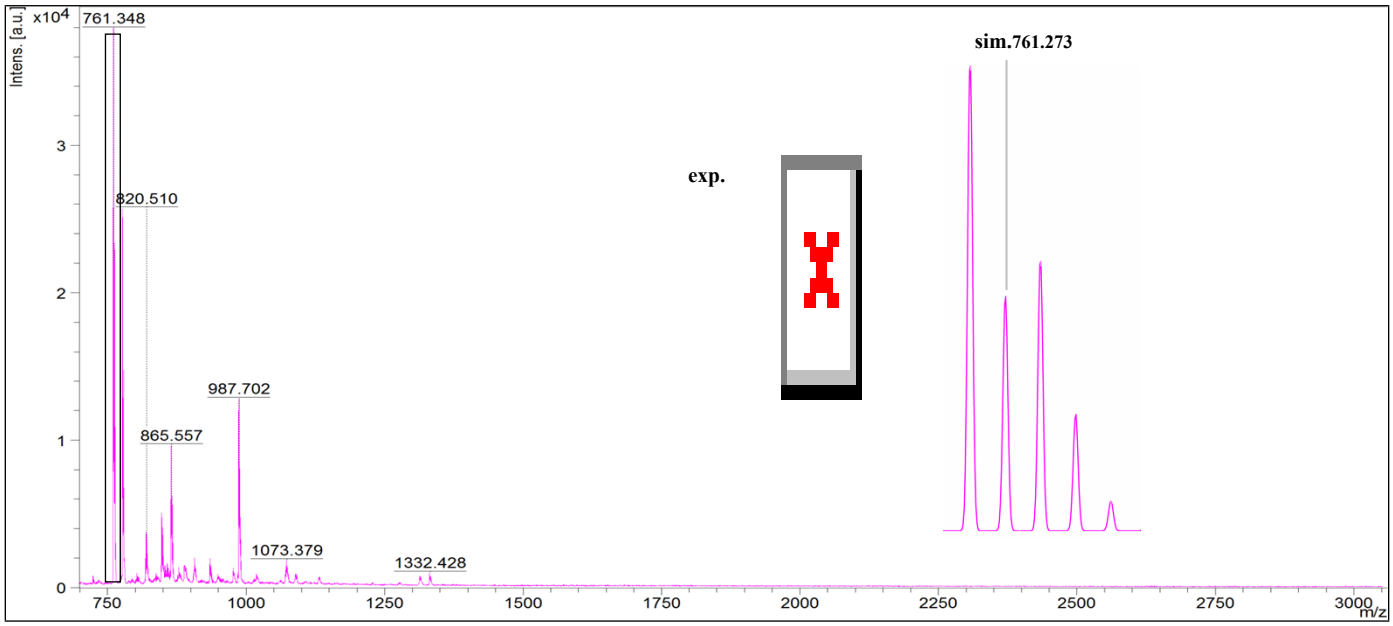

Fig. S9 MALDI-TOF Mass spectrum of **3b** (inset show the experimental and simulated isotopic pattern for $[M]^+$**).**

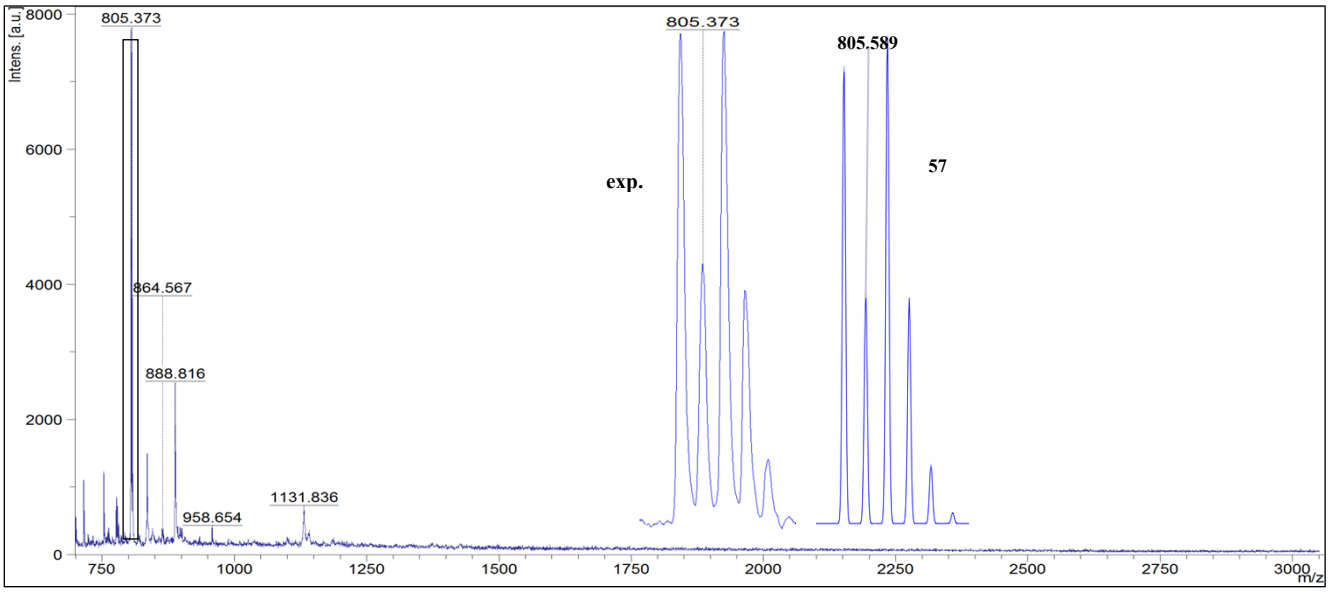

Fig. S10 Hill plot of **2** with addition of **(a)** TFA **(b)** TBAOH.

(a)

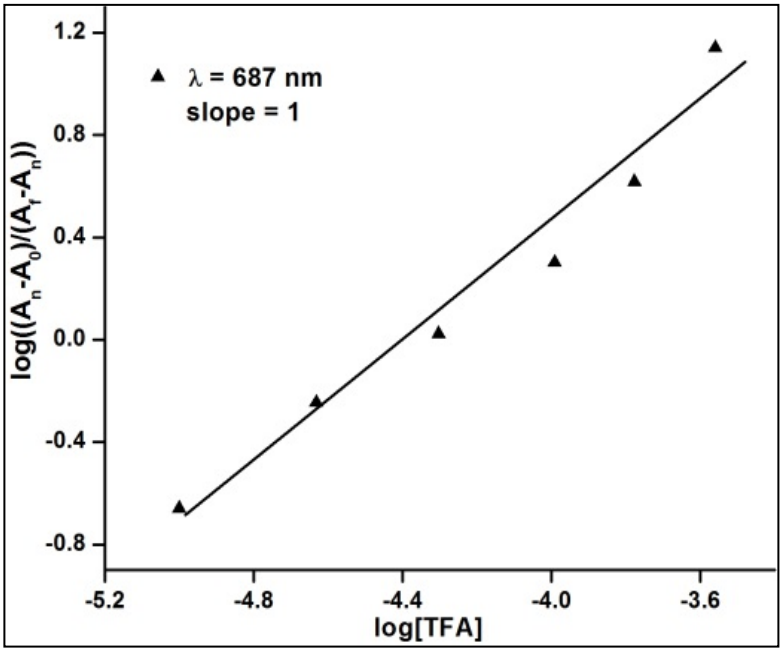

(b)

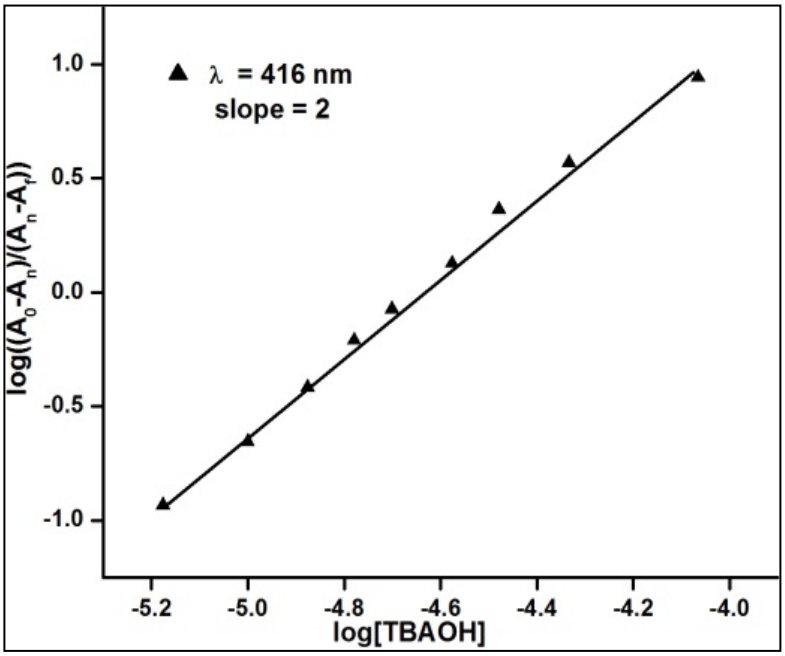

Fig. S11 (a) Protonation studies of **3** using TFA in CH_3CN (inset shows plot [TFA] versus $[TFA]/A_n\text{-}A_0$.) **(b)** Hill plot, protonation of **3**.

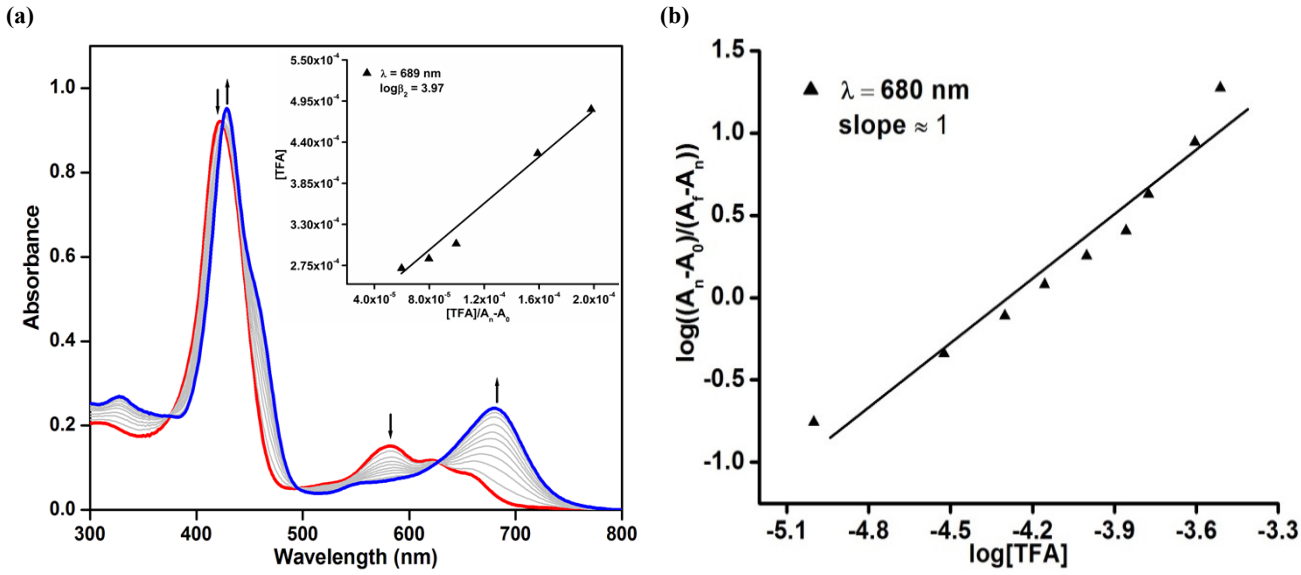

Fig. S12 (a) Deprotonation studies of **3** using TBAOH in acetonitrile, inset shows plot between $[TBAOH]^2$ and $\{TBAOH]^2/A_n$-A_0. (b) Hill plot, deprotonation of **3.**

(a)

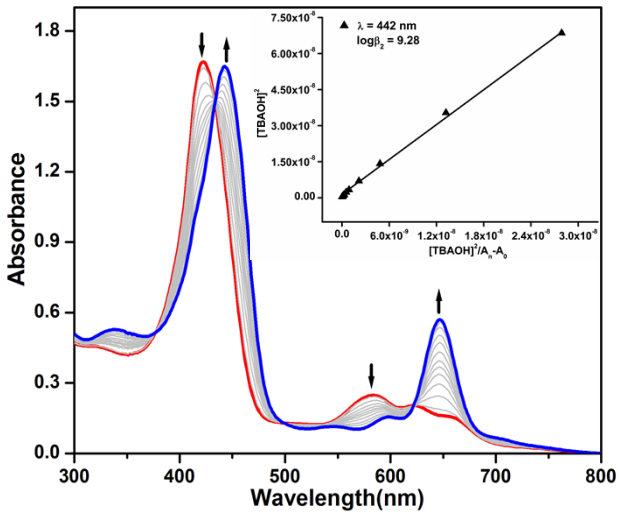

(b)

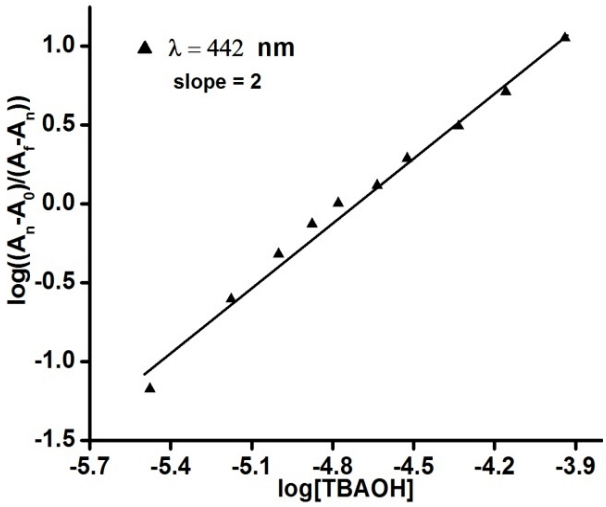

Fig. S13. Electronic absorption spectral changes in **2** (a) while addition of various anions in CH_3CN and (b) Hill plot of **2** while adding of TBAF.

(a)

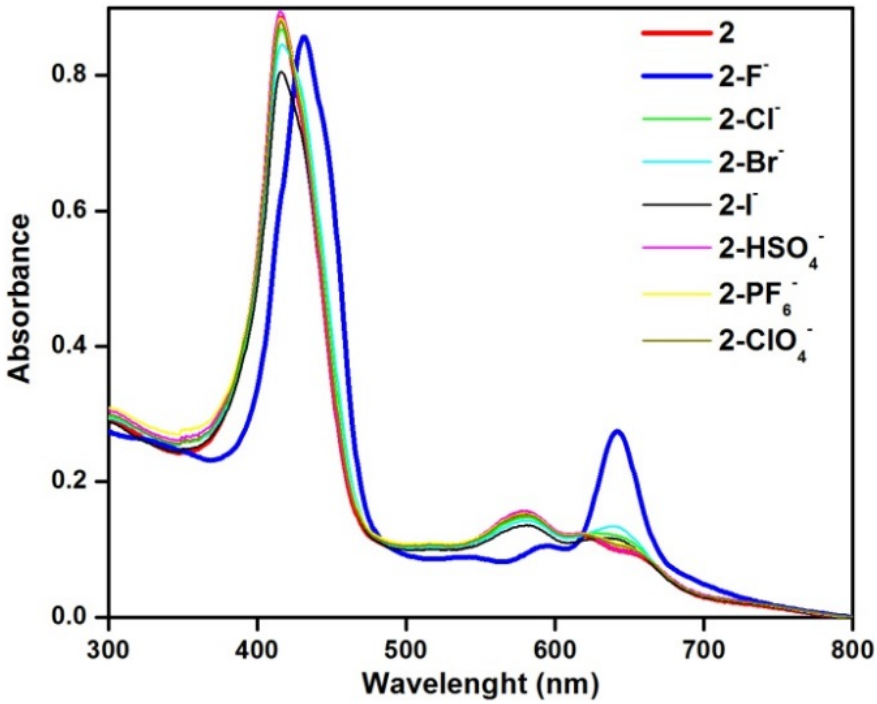

(b)

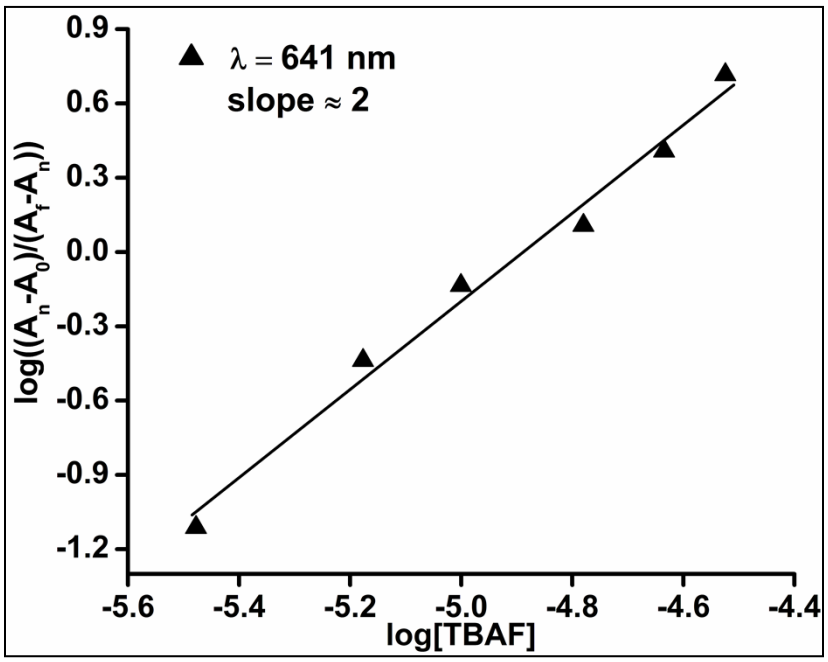

Fig. S14 UV-Visible spectral changes of **2** while addition (a) TBAOAc (inset shows plot [TFA] versus [TFA]/A_n-$A_{0.}$), (b) Hill plot for acetate binding with **2**.

(a) **(b)**

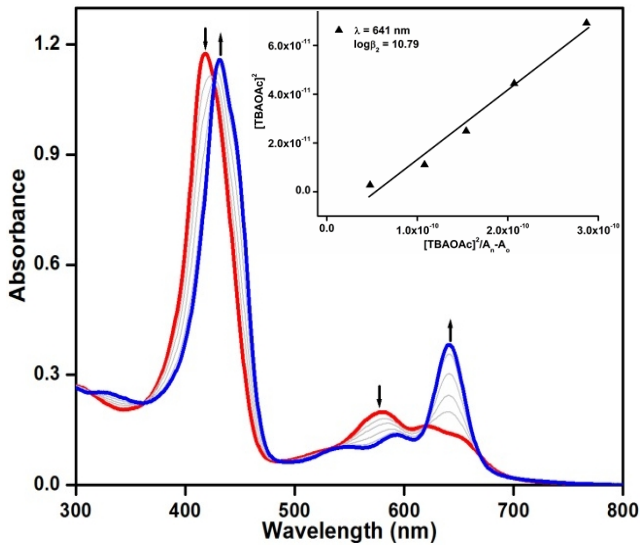

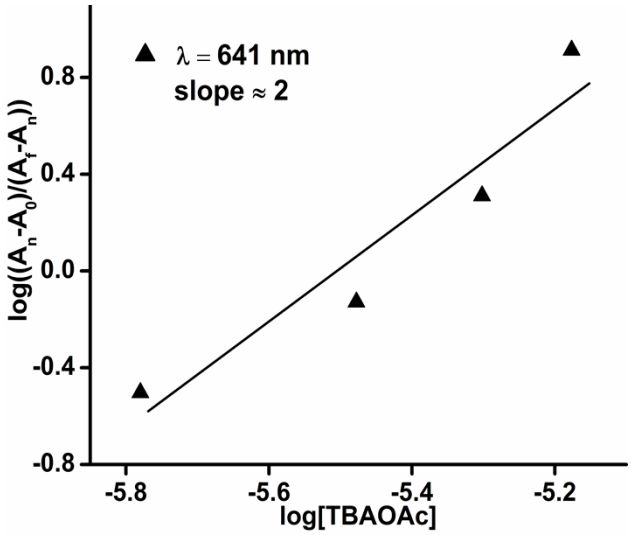

(c) with addition of $TBAH_2PO_4$ (inset shows plot [TFA] versus [TFA]/A_n-$A_{0.}$), and **(d)** showing Hill plot for dihydrogenphosphate binding with **2**.

(c) **(d)**

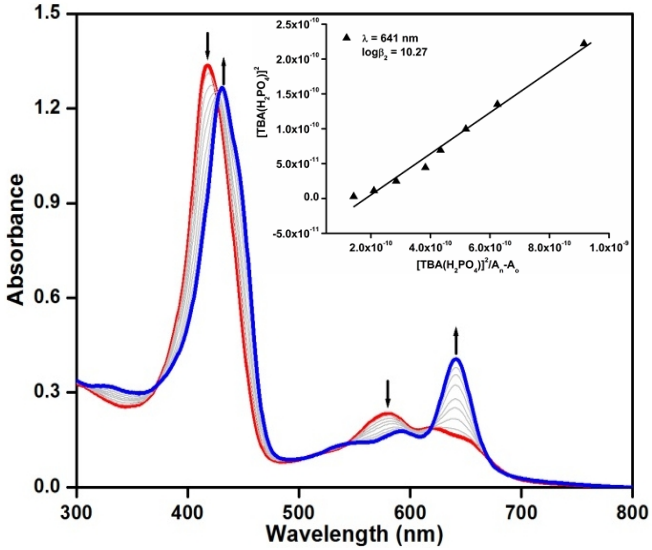

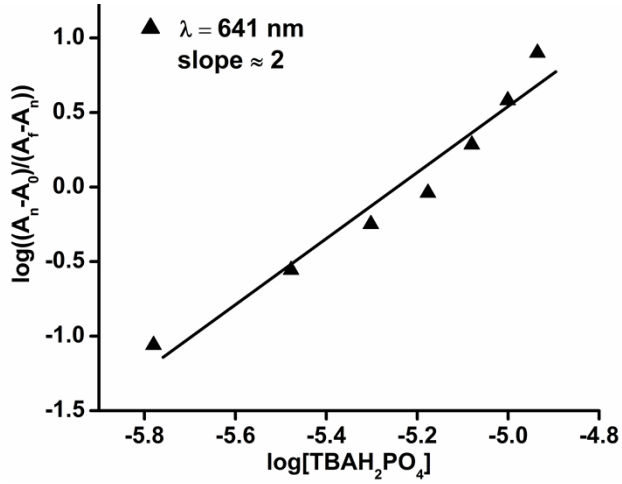

Fig. S15 (a) Electronic absorption spectral changes in **3** while addition of various anions in CH_3CN, (b) UV-Visible titration of **3** with fluoride ion in CH_3CN inset shows a plot $[TBAF]^2$ versus $[TBAF]^2/A_n\text{-}A_0$ for F^- ion binding with **3 (c)** Hill plot for F^-ion binding with **3**.

(a)

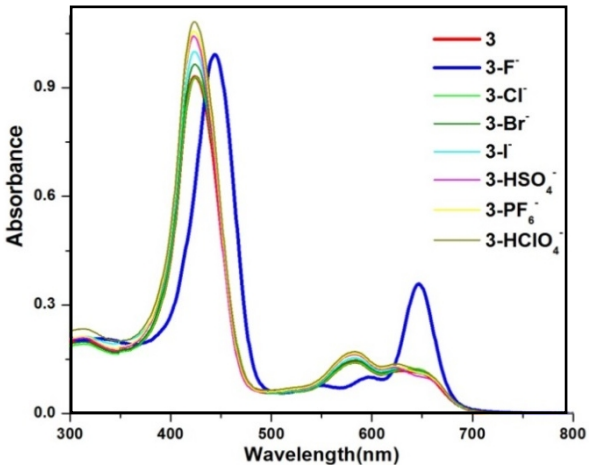

(b)

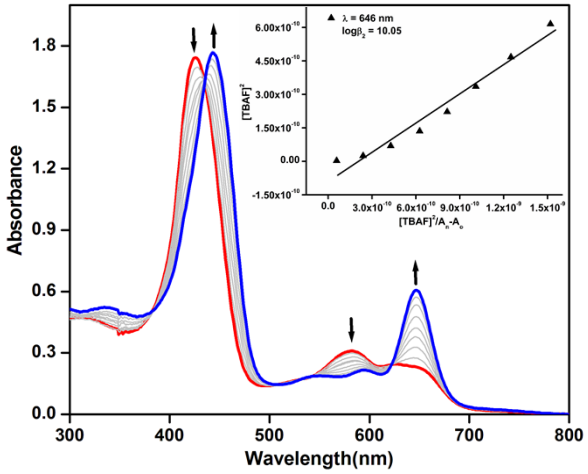

(c)

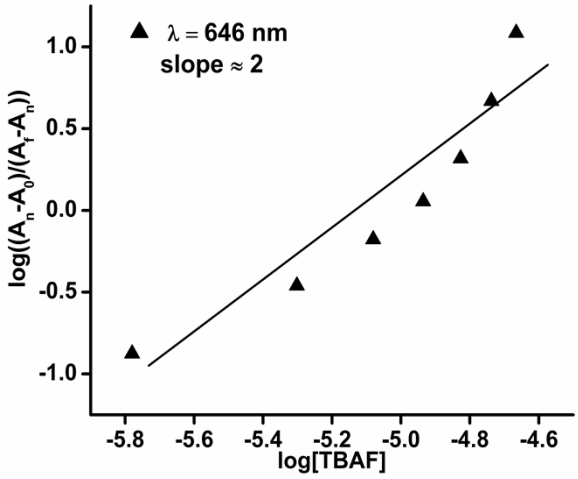

Fig. S16 UV-Visible spectral changes of **3** in CH_3CN **(a)** with addition of TBAOAc inset show plot $[anion]^2$ *versus* $[anion]^2/A_n$-A_o **(b)** Hill plot

(a)

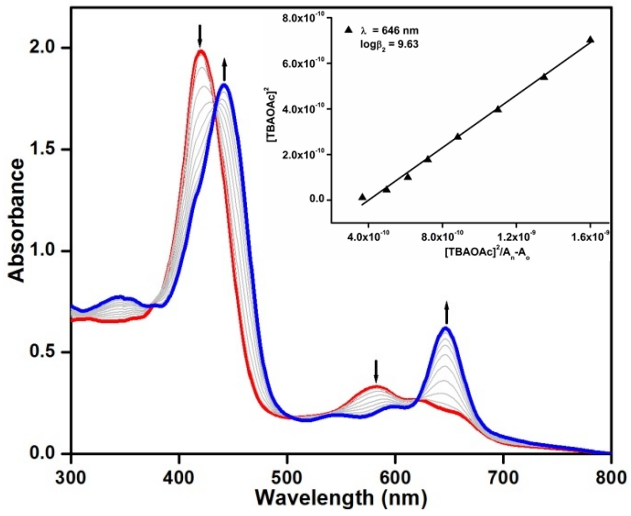

(b)

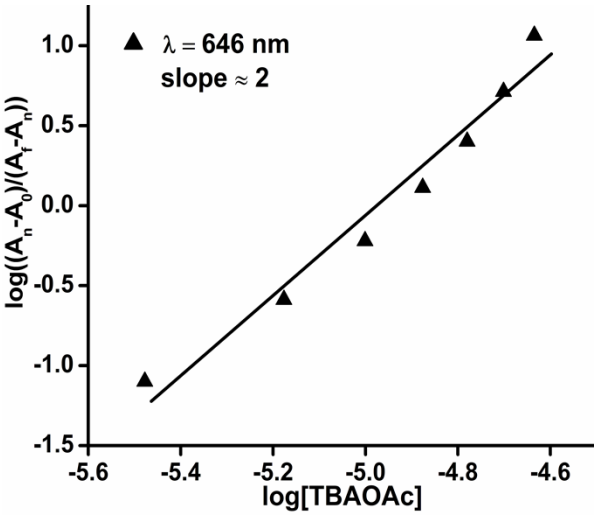

(c) while addition of $TBAH_2PO_4$ inset show plot $[anion]^2$ *versus* $[anion]^2/A_n$-A_o **(d)** Hill plot

(c)

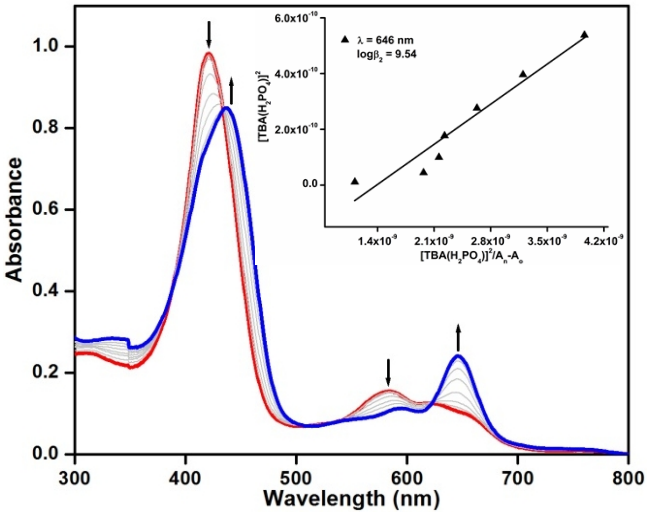

(d)

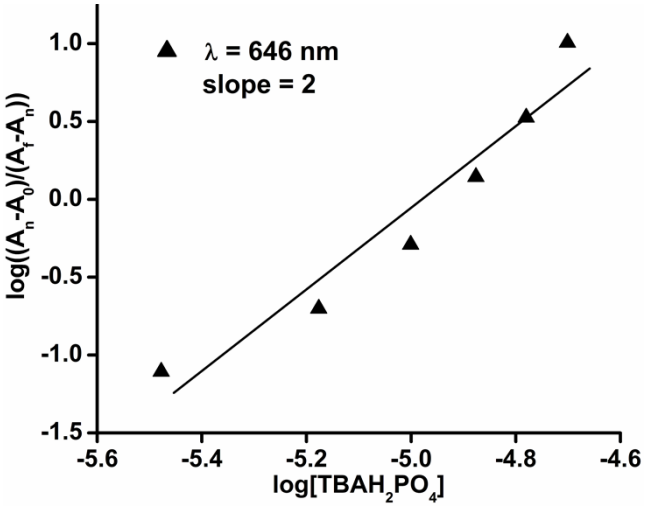

Fig. S17 Absorption spectral changes while addition of fluoride and MeOH with **2** in CH_3CN.

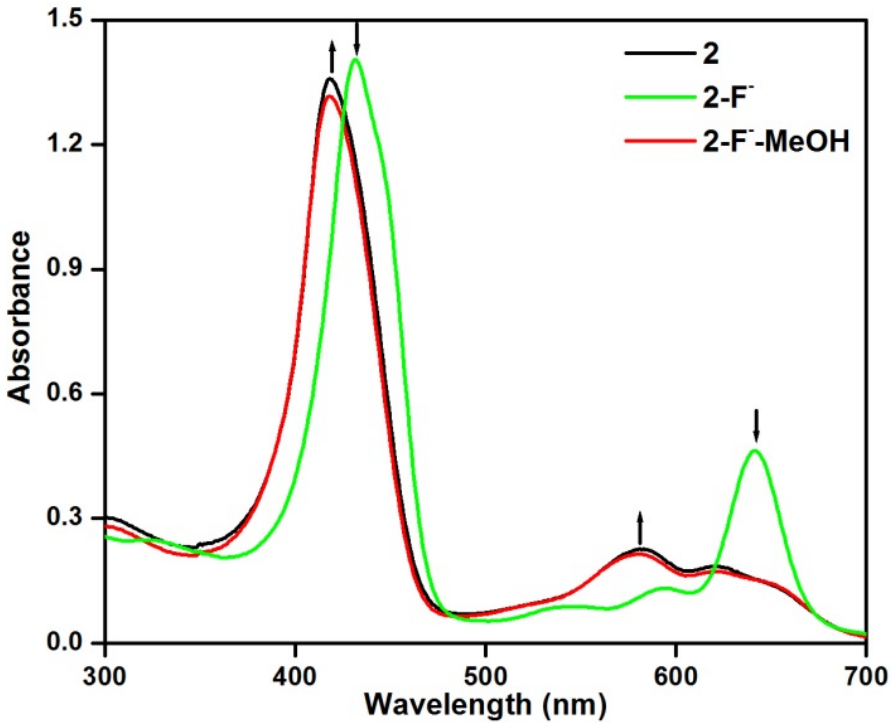

Fig. S18 Cyclic Voltammograms of free base **1-3** corroles in CH_2Cl_2 containing 0.1M TBAP (with a scan rate of 100 mV/s. GC Working electrode, Ag/AgCl Reference electrode and Pt wire counter electrode were used).

corrole	3σ	Oxidation		Reduction
		I	II	I
1	0	630	1024	-1300[a]
2	1.59	747	-	-893[a]
3	1.35	740	1196	-1137[a]

[a]Irreversible reduction potential.